Characterisation of track buckling resistance

Citation for the original published paper (version of record):
Kabo, E., Ekberg, A. (2024). Characterisation of track buckling resistance. Proceedings of the Institution of Mechanical Engineers, Part F: Journal of Rail and Rapid Transit, 238(7): 786-794. http://dx.doi.org/10.1177/09544097241231884

Published as
Elena Kabo & Anders Ekberg, Characterisation of track buckling resistance, Proceedings of the Institution of Mechanical Engineers, Part F: Journal of Rail and Rapid Transit (2024). Copyright © 2024 by Institution of Mechanical Engineers .
DOI: https://doi.org/10.1177/09544097241231884.

Characterisation of track buckling resistance

Elena Kabo & Anders Ekberg*

Chalmers University of Technology

CHARMEC / Division of Dynamics

SE 412 96 Gothenburg

SWEDEN

elena.kabo@chalmers.se anders.ekberg@chalmers.se

Keywords: Thermal buckling, railway track, parametric influence, numerical simulations, data analysis, failure reports

Abstract

The study sets out with a network-wide analysis of the risk for track buckling that concludes that track buckling relates to a few "weak points" along the track. To identify these, a numerical model to predict track buckling resistance is developed. The influences of key track parameters are evaluated and quantified using the innovative concept of an equivalent temperature. This allows to quantify the large influence of e.g., curves and hanging sleepers in terms of an equivalent increase in temperature. Influence of less well-defined track parameters such as nearby fixed points or recent track work is estimated through statistical assessment of track buckling reports. Predicted influence generally agrees with empirical knowledge with some exceptions that are discussed in the report. Developed models and produced results should be valuable in identifying track sections at risk of track buckling and in assessing effectiveness of mitigating actions.

1 Introduction

Track buckling is a phenomenon where the restricted thermal expansion of a rail induces high compressive forces that causes the track structure to buckle. In jointed tracks, track buckling is prevented by expansion joints that allow some (moderately resisted) expansion. On the other hand, the buckling resistance is low once the thermal expansion exceeds the width of the expansion joints, and the entire compressive force must be carried by the track structure. In contrast, continuous welded tracks have no expansion joints, but compensate with a (much) higher buckling resistance of the

* Corresponding author

track. The extreme cases here are slab track constructions where the resistance to track deflection is very high.

To clarify the importance of straightness and lateral stiffness of the track, consider a perfectly straight 60E1 rail [1] that is completely translationally fixed at the fastenings (sleeper spacing *L* = 65 cm). This will result in Euler buckling with a critical load of

$$P_{\mathrm{E2}} = \frac{\pi^2 EI}{L^2} = \frac{\pi^2 \cdot 210 \cdot 10^9 \cdot 5.12 \cdot 10^{-6}}{0.65^2} = 25.1 \text{ MN} \quad (1)$$

where *E* is the elasticity modulus, and *I* is the moment of inertia related to lateral bending. This corresponds to a temperature of some

$$\Delta T = \frac{P_{\mathrm{E2}}}{EA\alpha} = \frac{25.1 \cdot 10^6}{210 \cdot 10^9 \cdot 7.67 \cdot 10^{-3} \cdot 11 \cdot 10^{-6}} = 1418 \text{ °C} \quad (2)$$

where *A* is the cross-sectional area and α the coefficient of thermal expansion. As seen, track buckling is not an issue under such ideal conditions.

In real tracks there is a limited resistance to lateral (and vertical) deflections [2]. There are also initial geometrical deviations that cause track buckling to progress more as a gradually increase in deflection than as a pure limit load phenomenon. For this reason, it is vital to be aware of the employed definition of track buckling when analysing the operational frequency. As an example, the Swedish infrastructure manager Trafikverket classifies a local track geometry irregularity as a track buckling event if there is a lateral track shift of at least 25 mm measured over 10 m, while – at the same time – there are high compressive forces in the track due to heat [3].

In the literature, there are several studies devoted to track buckling. Extensive overviews are presented in [4, 5] and references therein. There are also investigations related to more specific effects. As examples, the influence of sleeper shape was investigated in [6] using numerical simulations, and in [7] using both experiments and simulations. In [8] the influence of ballast fouling was investigated through finite element simulations that featured lateral track resistance for fouled ballast estimated from discrete element simulations. Finite element analyses have also been employed to study the effect of mixed timber and concrete sleepers [9].

The aim of the current study is to quantify the effect of local track conditions to the buckling resistance of the track. This knowledge can be employed to identify track sections with the highest risk of buckling and quantify effects of maintenance actions that improve local track conditions. To this end, both numerical simulations, and statistical analyses of operational track buckling events are employed. The quantification of the severity of different conditions is based on the innovative concept of an equivalent temperature, as described in section 3.2. Note that the focus is on the track resistance to buckling. The situation will also be aggravated by operational loading from vehicles entering the deformed track section [10]. This is however outside the scope of the current study.

2 Network-wide assessment of the risk of track buckling

To roughly assess the overall statistical risk of track buckling, correlation between number of (verified) track buckling events, and the maximum (ambient) temperature over a year was investigated. These data are presented in Figure 1.

The railway network managed by Trafikverket consists of about 14 200 kilometres of track. Presume that the resistance of the track varies between these sections such that if the ambient temperature exceeds a critical value T_c a track buckle will form in that kilometre section. Further presume that T_c is a statistical parameter that follows a normal distribution with an average value μ_c and a standard deviation σ_c. Selecting μ_c and σ_c to minimize the (root-square) deviation between predicted and actual number of track buckles in Sweden yields μ_c = 70.8°C and σ_c = 14.4°C. In other words – if this analysis is to be trusted – a temperature in Sweden of 71°C would result in a track buckle every second kilometre (since the risk of track buckling per kilometre is then 0.5). Predicted and occurring track buckles for all studied years are presented in Figure 1.

Year	08	09	10	11	12	13	14	15	16	17	18	19	20	21
Max temp	33	32	35	34	32	31	35	33	33	28	35	35	34	35
No of buckles	82	64	51	65	27	56	115	47	63	18	198	55	63	53

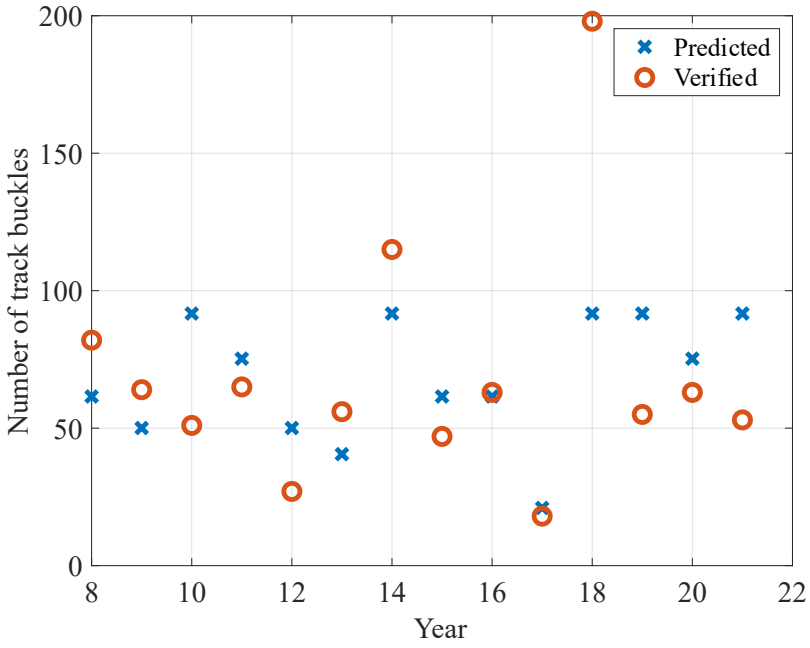

Figure 1 a) Maximum temperatures over the year (from annual and seasonal summaries at smhi.se) and number of confirmed track buckling events (from Trafikverket's annual summaries, see [11]). b) Predicted and verified numbers of track buckles in Sweden 2008 to 2022.

Figure 1 shows that the prediction is rough – a peak temperature of 35°C has led to between 51 and 198 track buckling events, whereas the predicted number is 92. Still some qualitative conclusions can be drawn: The average strength of the track (defined here as the temperature that can be sustained over a one-kilometre section of the track without resulting in a track buckle) is around 70°C. Consequently, track buckling does not relate to an "average" track, but to "weak" points along the track. The strength of the "weakest" points is in the predictive model quantified by μ_c and σ_c. Increasing μ_c by 5°C would decrease the predicted number of track buckles at 35°C from 92 to 33. The same effect is obtained by reducing σ_c by 1.8°C. Increasing μ_c can be obtained by increasing the stress-free temperature – the temperature at which there are no thermally induced forces in the rail. This would have the side effect of increasing the risk of rail breaks in the winter [12]. Decreasing σ_c relates to reducing influence of factors such as curves, poorly supported sleepers etc. To better understand the influence of such factors, a much more refined analysis is required. To this end numerical simulations will be employed.

3 Numerical analysis of track buckling

To analyse the influence of individual parameters on track buckling resistance, a numerical model was constructed. The model includes a span of 100 sleepers with fixed rail ends. Rail and sleepers are modelled as elastic beams. The fastenings (including rail pads) and ballast resistance are modelled as springs. Since the buckling resistance of the track is investigated, the loading consists only of heating and cooling of the rail in addition to the gravitational loading. The numerical model is visualized in Figure 2a.

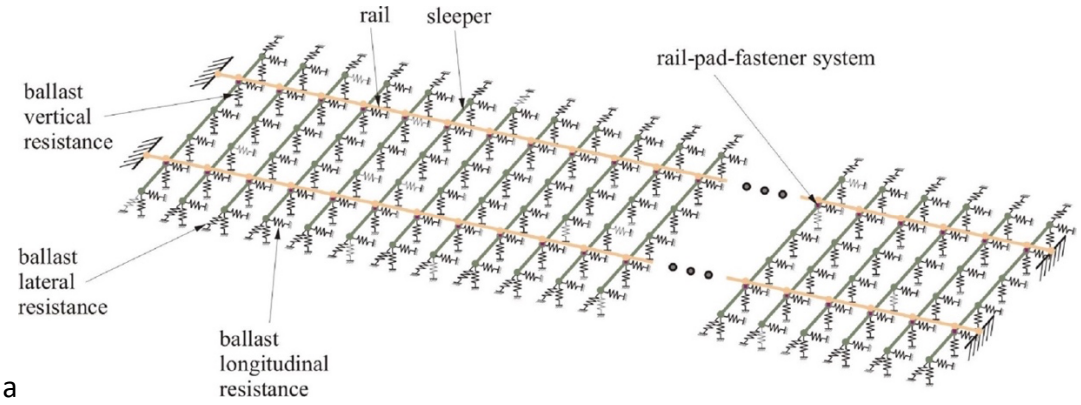

a

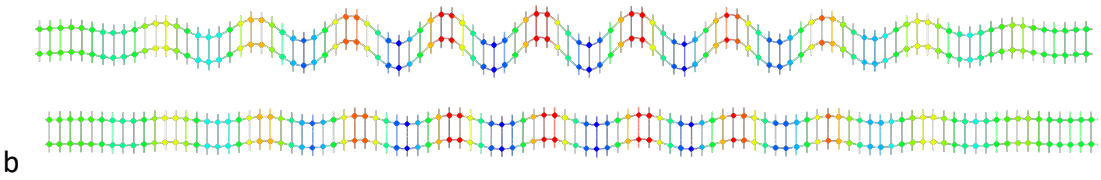

Figure 2 Track buckling model. a) Schematics of the numerical model for analysis of track stability. b) Buckling mode of the nominal reference track configuration (top) and deformed shape of the thermally loaded track (bottom).

The buckling analysis consists of two steps:

In the first step the buckling mode of the track structure is evaluated (see top picture of Figure 2b) and normalized so that the largest initial displacement equals d_{irr}.

In the second step, this irregularity is imposed on the nominal track geometry, and post-buckling analysis following the Riks method [13] is carried out as the rail temperature is gradually increased (bottom picture of Figure 2b).

If the track response is linear, and nominal and distorted track characteristics are the same (except for the track irregularity employed as a scaled buckling mode), the deformed shape will be identical between the two cases. The buckling mode is symmetric with a sinusoidal deformation pattern (cf. buckling of a beam supported by an elastic bed).

It could be argued that actual track geometry should be used as the initial irregularity. However, for the current study of parametric influence this is not feasible since the actual track geometry is the consequence of local variations in track stiffness and resistance that would then need to be quantified and incorporated into the model.

3.1 Reference configuration

For the numerical simulations, a reference configuration is defined that features:

- Tangent track with an initial lateral irregularity of d_{irr} = 5 mm, see Figure 2a. The rather high value reflects the fact that track buckling occurs only in the very worst track sections.
- Nominal 60E1 rails
- Track stiffness is estimated as k_x = 0.49, k_y = 1.9, k_z = 35.7 [MN/m] in the longitudinal, lateral, and vertical directions, respectively. In the Riks-analysis an elastoplastic ballast element described in [14] is employed with stiffnesses k_x = 3.5, k_y = 5.0, k_z = 100 [MN/m].
- Fastenings with estimated stiffnesses k_x = 5.25, k_y = 26.3, k_z = 100 [MN/m], k_{xy} = k_{yz} = k_{xz} = 16.6, [N/rad].
- Concrete sleepers, see [2]

Initial simulations were employed to ensure that the results (in terms of equivalent temperatures, see section 3.2) were not significantly affected by boundary conditions or mesh density.

3.2 Equivalent temperature evaluation

To interpret simulation results, differences in temperature increases required to obtain lateral deflections of 2.5 mm and 5 mm (in the following denoted $\Delta T_{2.5}$ and $\Delta T_{5.0}$ and measured in degrees Celsius) between the studied cases and the reference case (defined above) were introduced, see Figure 3. These measures represent the equivalent temperature increase of the studied modifications. In other words, if a reduced stiffness corresponds to $\Delta T_{5.0}$ = 10°C, then a lateral displacement of 5 mm (in addition to the initial irregularity) will be obtained in the reference configuration if the temperature is 10°C higher than in the modified configuration.

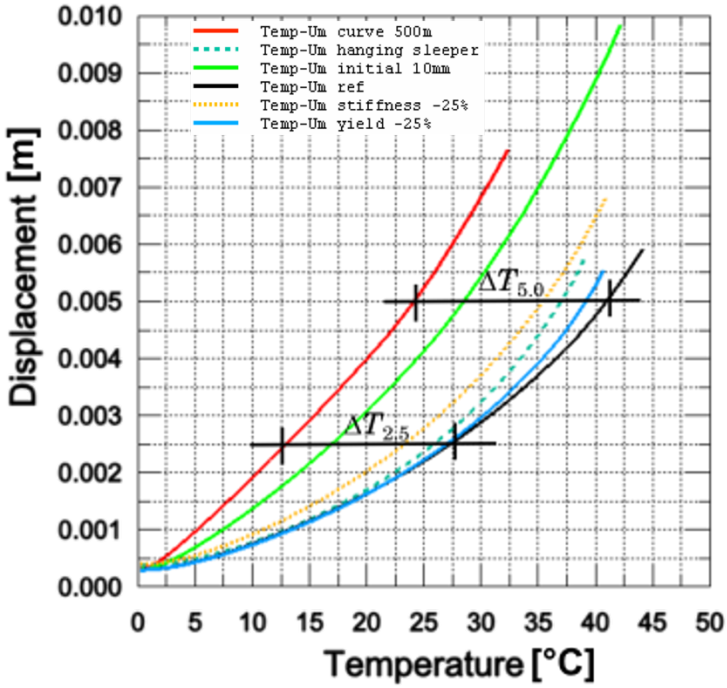

Figure 3 Definition of the measures $\Delta T_{2.5}$ and $\Delta T_{5.0}$ for the load case represented by the red curve. The reference case is the black curve to the right. In the legend "yield" relates to the elastoplastic ballast element employed in the Riks-analysis.

4 Influence of key parameters

Through numerical simulations, the influence – in terms of equivalent temperatures – of some key parameters are investigated. The key parameters, and the investigated magnitudes different from those of the reference case are

- Curve radius – 150, 250, 350, 500 and 800 m.
  The curves feature the same magnitude of irregularities as the reference case.
- Hanging sleepers – 1, 3 and 5 hanging sleepers.
  These adjacent sleepers do not feature any lateral support.
- Lateral ballast stiffness – reductions in lateral ballast stiffness of 25% and 50%
  Simulations showed (not surprisingly) that the lateral stiffness had much more influence than the vertical stiffness.

- Fastening stiffness – 50% and 75% overall decrease.
- Initial track irregularity, d_{irr} – 7 mm.
- 50E3 rail profile

The results of the parametric study are compiled in Figure 4. Note how a reduced ballast stiffness (globally and locally) will result in a steeper temperature–displacement relationship, as compared to the influence of a curve. The reason is that the curve radius will initially introduce a lateral force component. However, as the rail is displaced, this effect will gradually decrease. In contrast, the influence of a decreased ballast resistance will remain constant throughout the buckling process.

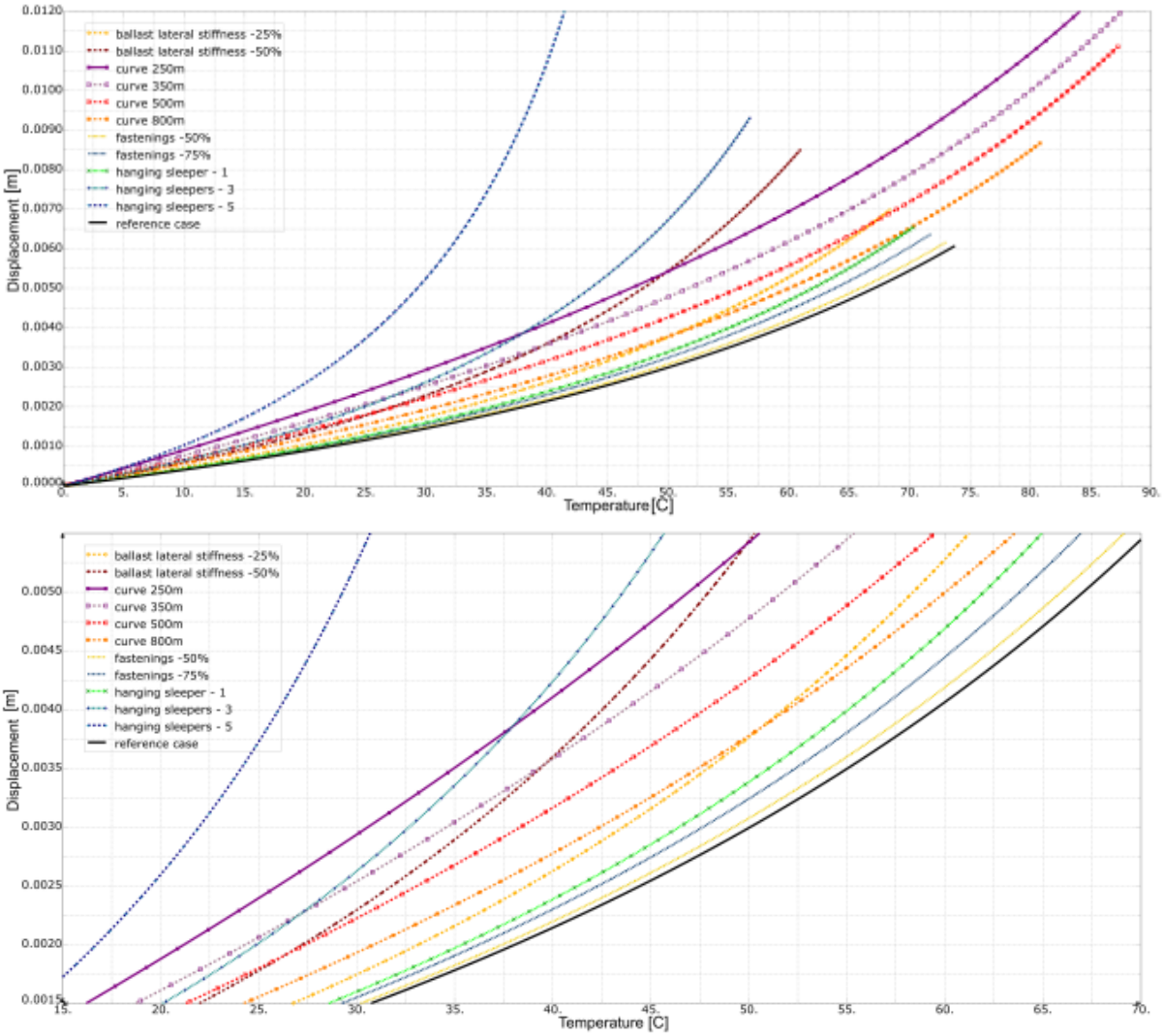

Figure 4 Evaluated temperature–displacement responses for different magnitudes of key parameters. Overview and zoom-in.

The results in terms of $\Delta T_{2.5}$ and $\Delta T_{5.0}$ are compiled in Table 1.

Table 1 Equivalent temperature increases $\Delta T_{2.5}$ and $\Delta T_{5.0}$ for the studied parameter variations.

Parameter variation	$\Delta T_{2.5}$ [°C]	$\Delta T_{5.0}$ [°C]
Lateral ballast stiffness –25%	6	9
Lateral ballast stiffness –50%	13	19
Curve 250 m	19	20
Curve 350 m	15	15
Curve 500 m	12	11
Curve 800 m	7	7
Fastening stiffness –50%	0.5	1
Fastening stiffness –75%	2	3
One hanging sleeper	3	5
Three hanging sleepers	16	25
Five hanging sleepers	25	38
Initial irregularity 7 mm, straight track	12	13
Initial irregularity 7 mm, 150m curve	5	3
50E3 rail, straight track	-2	-2
50E3 rail, 150m curve	2	2

Note that the influence of initial irregularity size and of the 50E3 rail in 150 m curves is in addition to the influence of the curve itself. Also note the slight *decrease* in equivalent temperature for the 50E3 rail on straight track due to the lower axial load resulting from the smaller cross-sectional area.

4.1 Estimations of the influence of hanging sleepers and curves

The results from the parametric study can be further analysed in a regression analysis. For the influence of hanging sleepers, this yields an estimate of the equivalent temperature increase as

$$\Delta T \approx -0.6 \cdot N^2 + 10 \cdot N - 6 \qquad (1)$$

where N is the number of hanging sleepers. This estimate together with simulation results, are presented in Figure 5a. Note that the curve is derived using both $\Delta T_{2.5}$ and ΔT_5 results since buckling of a track containing initial irregularities is a gradual phenomenon, which makes it difficult to say at which lateral deflection it has initiated. For the case of hanging sleepers the temperature–deflection curve is steeper than for the reference case, which makes the non-linearity more apparent.

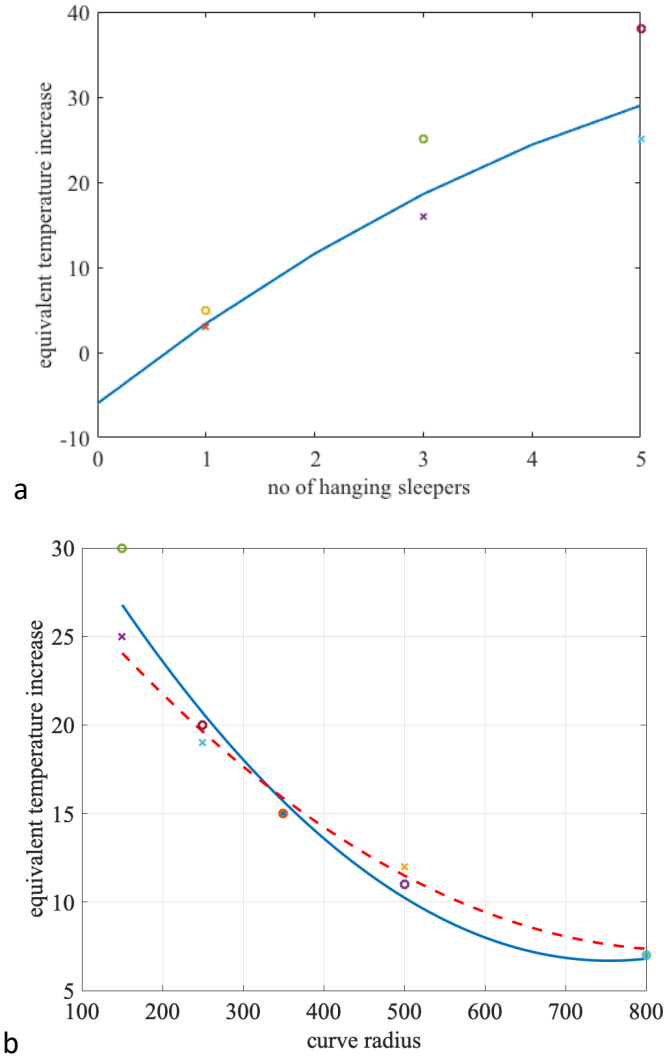

Figure 5 Simulated influence on equivalent temperature increases $\Delta T_{2.5}$ (x) and $\Delta T_{5.0}$ (o) of a) Hanging sleepers and estimate according to (1). b) Curve radius and estimates according to (2) (red, dashed) and (3) (blue).

The influence of a curve radii in the range 250 m to 800 m can be estimated as

$$\Delta T \approx 3.4 \cdot 10^{-5} \cdot R^2 - 0.058 \cdot R + 32 \qquad (2)$$

Here R is the curve radius in meters. The estimation together with simulation results are presented in Figure 5b.

For the influence of curve radii 150 to 250 m, a more conservative estimation is

$$\Delta T = 5.5 \cdot 10^{-5} \cdot R^2 - 0.083 \cdot R + 38 \qquad (3)$$

as also presented in Figure 5b.

4.2 Numerical predictions versus empirical estimations

The simulation results can be compared to regulations in [15], which define (experienced based) reductions in critical rail temperatures for track buckling. The comparison is presented in Table 2.

Table 2 Comparison of simulated equivalent temperature increases versus Network Rail reductions in critical temperatures [15].

Configuration	NR	$\Delta T_{2.5}$	$\Delta T_{5.0}$
Undisturbed (reference)	0	0	0
Unconsolidated (NR) vs overall stiffness reduction of 50%	17	13	19
No ballast at sleeper ends (NR) vs lateral stiffness reduction of 25%	17	6	9
No ballast at sleeper ends and sides (NR) vs lateral stiffness reduction of 50%	22	13	19
3 (or more (NR)) hanging sleepers	22	16	25
Radius below 400 metres (NR) vs 500 meter curve	9	12	11

The 25% and 50% ballast stiffness reductions are selected to reflect the fact that approximately one third of the lateral resistance comes from the sleeper bottom side, a second third from the sides and a last third against the shoulder when no vertical load is applied, see [16]. In the case of a loaded sleeper, the bottom of the sleeper should take more load, which motivates using values somewhat below 33% and 66%.

In general, the estimations based on simulation results show reasonable agreement with the NR empirical estimations. The latter are on the safe side with the exception of the influence of curves. It should however be noted that the simulations do not consider any widening of ballast shoulders as is commonly mandated in curves.

5 Comparison to occurring track buckling

To evaluate the relevance of the numerical simulation results, reports on track buckling on the Swedish network collected between April 2008 and September 2019[1] were scrutinized. Track buckling in curves with radii between 250 meters and 800 meters with reported rail temperatures above 10°C were considered. The distribution of curve radii for the 242 cases are presented in Figure 6a. Note the high proportion of sharp curves.

The corresponding distribution of measured rail temperatures are presented in Figure 6b.

[1] Compiled by Emelie Rennie and Fredrik Andersson at Trafikverket

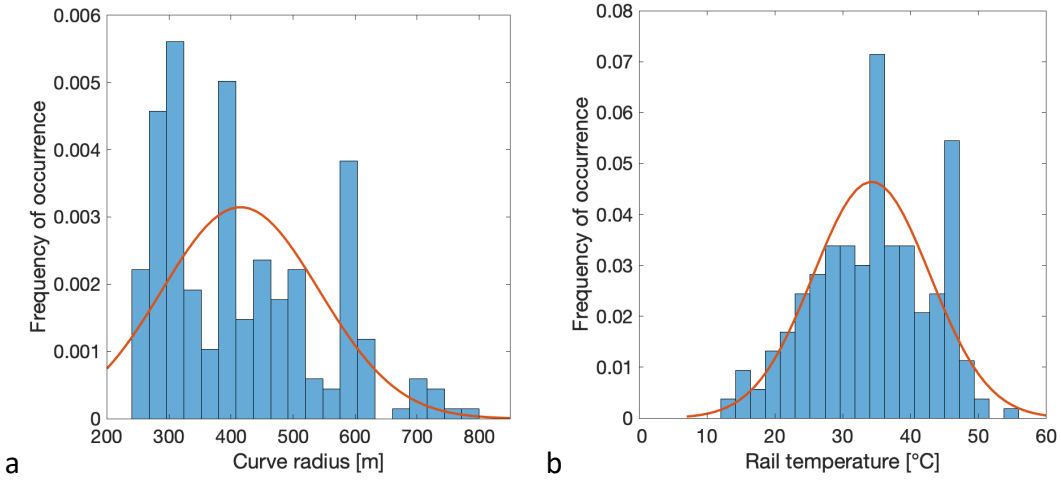

Figure 6 a) Distribution of curve radii in the range 250 m < *R* < 800 m for reported track buckling. b) Distribution of reported rail temperatures. Red lines indicate fitted normal distributions.

For the following analysis it is important to recall that if the track was completely uniform, all track buckling events would occur at the same rail temperature – the theoretical buckling load. Further, if influencing parameters not accounted for are independent, random and sum up to the total track resistance, the measured rail temperatures at buckling (i.e., when resistance is overcome) would follow a (nearly) normal distribution.

In the studied case there are influencing factors that cause scatter and a deviation from a normal distribution. The approach taken is to compensate for these factors and assess the compensation by the decrease in scatter and the improved resemblance to a normal distribution.

To estimate the scatter in rail temperatures, the coefficient of variation $\delta_x = s_x/\bar{x}$ for the sample of temperatures, x, is employed. Here, s_x is the standard deviation and $\bar{x}$ is the average. For the unmodified temperatures, $\delta_x = 0.25$.

To estimate the match towards a normal distribution, the Kolmogorov–Smirnov test as implemented in MATLAB [17] is employed. It defines the p-value as the probability of observing a test statistic as extreme as, or more extreme than, the observed value under the null hypothesis that the data comes from a standard normal distribution. Small values of p may indicate that the test data are not normally distributed.

5.1 Modifications for curve radius

The measured rail temperatures were modified for curvature according to equation (2) (using equation (3) for curves with radii below 450 m did not significantly alter the results). The corresponding modified rail temperature distribution is presented in Figure 7a. The corresponding coefficient of variation is $\delta_x = 0.20$.

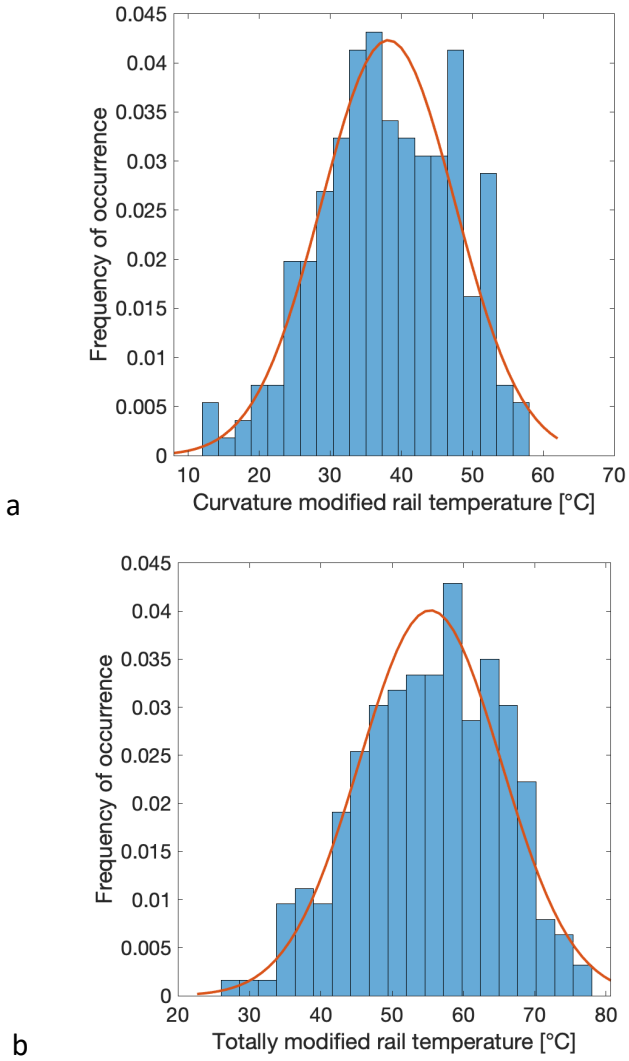

Figure 7 Distribution of rail temperatures modified with respect to a) Curvature according to equation 2, b) Curvature and other influencing parameters. The red lines indicate fitted normal distributions.

5.2 Modifications for other parameters

In addition to curve radii, also reported track work, lack of ballast, a fixed point in the vicinity of the track buckle, and wooden sleepers were accounted for. Temperature modifications with increases in the span 0 °C to 7 °C (with a step of 1 °C) for each of the influencing parameters were tested. A full analysis was carried out meaning all combinations of influences were evaluated. The minimum δ_x =0.18 was obtained for temperature modifications of

- Track work: +5°C
- Lack of ballast: +5°C
- Fixed point: +1°C

- Wooden sleeper: +3°C

The distribution of modified temperatures is presented in Figure 7b.

5.3 Quality of compensation for the various influencing factors

In Table 3, quantities of the un-modified and modified (with respect to curvature, track work, lack of ballast, fixed point and wooden sleepers) fitted normal distributions are presented.

From comparing Figure 6b and Figure 7 and the characteristics in Table 3, it is clear that the modification decreases the scatter in rail temperatures. It also makes the rail temperature more normal distributed. As discussed above, a normal distribution is what should be expected if all parameters that have a systematic influence are correctly compensated for.

Table 3 Characteristics of modified and unmodified distributions of rail temperatures.

	un-modified	**modified**
average ($\bar{x}$) with 95% confidence limits	33.2 34.3 35.4	54.1 55.4 56.6
standard deviation (s_x) with 95% confidence limits	7.9 8.6 9.4	9.14 10.0 10.9
coefficient of variation (δ_x)	0.25	0.18
normalised average ($\bar{x}$) with 95% confidence limits	0.97 1 1.03	0.98 1 1.02
normalised (s_x) with 95% confidence limits	0.92 1 1.10	0.92 1 1.10
p -value	0.42	0.77

6 Discussion

The influence of various parameters on decreased track buckling resistance has been assessed through numerical simulations and statistical analyses of track buckling reports. The numerical simulations quantify the influence of curves, hanging sleepers, track irregularities etc. The influence is shown to be in line with empirical findings.

The presumption in the statistical analysis is that a correct compensation will correspond to a normal distributed rail temperature at track buckling with a decreased temperature scatter between buckling events. Here, scatter is quantified by the coefficient of variation δ_x, which is not ideal since a uniform increase in average temperatures (while keeping scatter constant) would itself lead to a lower δ_x. On the other hand, using the standard deviation s_x would be even more misleading since it would increase with uniformly increased temperatures.

As seen from the presented results, the compensations improve the situation, but does not fully compensate for all rail temperature variations. There are a number of reasons why this will never be the case. Some of these are:

- The list of considered factors is not complete. Two important factors that vary between buckling events and are not considered are track irregularities and operational loading from passing train at the time of the track buckling event. The influence on track irregularities has been assessed in the numerical simulations and could be accounted for if data of the condition just before the buckling event were known. The train load at the time of track buckling does however not relate to the track resistance and is therefore considered out of scope of the current investigation even if it will for sure affect the (magnitude of) buckling.
- The amount of influence of some factors is not included. As an example, all cases of track works are given the same temperature compensation.
- Actual rail temperatures are not measured at the exact time of rail buckling but during the following inspection (or have been estimated).

Note also that the severity of the buckling event is not considered. Instead, the evaluation treats all reported track buckling cases as equal.

With these reservations, it is interesting to see that there is a clear trend towards a normal distribution as temperature modifications are applied. The relatively low influence of wooden sleepers is somewhat surprising since tracks with continuously welded rail on wooden sleepers with "heyback" fastenings are known to be significantly over-represented regarding track buckling. A reason could be that for the cases studied there are so many cases of wooden sleepers that the effect is not carried through as an additional factor.

Similarly, the numerical simulations indicate a small influence of fastening stiffness, which may be caused by the rather crude representation of fasteners by springs in the simulation model. Such a representation does for example not account for play in a worn "heyback" fastening, which could reduce the resistance significantly.

The predicted influence of a fixed point is also small. This may be surprising since more than 50% of the track buckling events were reported to occur in the vicinity of a fixed point. It should however be noted that any fixed point (switch and/or crossing, bridge, road crossing, platform or other construction) closer than 100 meters from the track buckling should be reported with no consideration of the distance [3].

The influence of track work has been investigated in the literature. A summary of the existing literature [18] indicated a reduction in lateral ballast resistance of about 50% directly after tamping and around 20% after a month. The estimated temperature increase for track works, and for lack of ballast (ΔT=5 °C) would each correspond to some 20% reduction in lateral stiffness or one hanging sleeper (see Table 1), which seems like a reasonable influence.

7 Conclusions

A numerical model to simulate track buckling has been developed. The influence of key track parameters on the track resistance has been evaluated and quantified using the innovative concept of an equivalent temperature. Comparisons between the predicted influence and empirical reduction factors show good agreement. A possible exception is the influence of fastenings where the rather crude numerical modelling of these may be the cause.

The influences of operational parameters difficult to include in the numerical simulations have been estimated through modifications of measured rail temperatures from track buckling reports. The assumption here is that the modification with the best reflection of the influence would result in a narrow Gaussian distribution of track buckling temperatures. The predicted influence matched empirical knowledge well with the exception being wooden sleepers where it is believed that the common occurrence of these in buckling events prevents their relative influence to be carried through.

The developed analysis models and the evaluation results are believed to be valuable tools in identifying track sections at risk of track buckling, and the effectiveness of different mitigating actions.

Acknowledgements

Evaluated track buckling report data were compiled by Emelie Rennie and Fredrik Andersson at Trafikverket. The work is part of activities within the Centre of Excellence CHARMEC (www.chalmers.se/charmec). They are funded within the European Union's Horizon 2020 R&I programme in Shift2Rail projects In2Track2 and In2Track3 under grant agreements No.826255 and 101012456, and the Horizon Europe R&I programme in Europe Rail projects IAM4RAIL under grant agreement No. 101101966.

References

1. CEN. *Railway applications. Track. Rail. Vignole railway rails 46 kg/m and above*. Europeean Committee for Standardization, 2011. Report No.:13674-1:2011

2. Kabo E. A numerical study of the lateral ballast resistance in railway tracks. *Proc IMechE, Part F: J Rail and Rapid Transit* 2006; 220(4): 425–433.

3. Trafikverket, *BVR 1586.12 – Solkurvor - rapportering* (in Swedish), Report TDOK 2014:0667, 2015

4. Kish A and Samavedam G. *Track buckling prevention: theory, safety concepts, and applications*. John A. Volpe National Transportation Systems Center (US), Report No. DOT/FRA/ORD-13/16. 2013.

5. Pucillo G P. Thermal buckling and post-buckling behaviour of continuous welded rail track. *Vehicle System Dynamics* 2016; 54(12): 1785–1807.

6. Zakeri J A, Esmaeili M, Kasraei A, Bakhtiary A. A numerical investigation on the lateral resistance of frictional sleepers in ballasted railway tracks. *Proc IMechE, Part F: J Rail and Rapid Transit* 2016; 230: 440–449.

7. Miri A, Zakeri J A, Thambiratnam D, Chan T H T. Effect of shape of concrete sleepers for mitigating of track buckling. *Construction and Building Materials* 2021; 294: 123568.

8. Ngamkhanong C, Kaewunruen S, Baniotopoulos C. Influences of ballast degradation on railway track buckling. *Engineering Failure Analysis* 2021; 122: 105252.

9. Ngamkhanong C, Kaewunruen S, Baniotopoulos C. Nonlinear buckling instabilities of interspersed railway tracks. *Computers & Structures* 2021; 249: 106516.

10. Miri A, Dhanasekar M, Thambiratnam D, Weston B, Chan T H T. Analysis of buckling failure in continuously welded railway tracks. *Engineering Failure Analysi*s 2021; 119: 104989

11. Trafikverket. *Solkurvor 2021 - Statistik, analys och handlingsplan* (in Swedish). Trafikverket; 2022. Report TRV 2022/69997

12. Deuce R, Ekberg A and Kabo E. Mechanical deterioration of wheels and rails under winter conditions-mechanisms and consequences. *Proc IMechE, Part F: J Rail and Rapid Transit* 2019; 233(6): 640–648.

13. Riks E. An incremental approach to the solution of snapping and buckling problems. *Int J Solids and Structures* 1979; 15(7): 529–551.

14. Jacobsson L. *A plasticity model for ballast resistance*. SP Swedish National and Testing and Research Institute; 2005. Report No. 2005:27

15. Network Rail. *Managing track in hot weather*. Network Rail; 2021. Report No.:NR/L2/TRK/001/mod14 issue 7.

16. Miura S. Lateral track stability: theory and practice in Japan. *Transportation Research Record*; 1991. 1289: 53–63.

17. Mathworks. One-sample Kolmogorov–Smirnov test. https://se.mathworks.com/help/stats/kstest.html (accessed 16 March 2023).

18. Kabo E, Ekberg A and Jacobsson L. *Railway track stability – a state-of-the-art survey*. Chalmers Applied Mechanics; 2004. Research report 2004:2.